Multi-Vehicle Oceanographic Feature Exploration

B. H. Ooi, H. Zheng*, H. Kurniawati*, W. Cho*[†], M. H. Dao[‡], J. Wei*[§], P. Zemskyy[‡], P. Tkalich[‡], P. Malanotte-Rizzoli*[§], N. M. Patrikalakis*[†]*

*Singapore-MIT Alliance for Research and Technology Centre

[†]Center for Ocean Engineering, Department of Mechanical Engineering, Massachusetts Institute of Technology

[‡] Tropical Marine Science Institute, National University of Singapore

[§]Department of Earth, Atmospheric and Planetary Sciences, Massachusetts Institute of Technology

ABSTRACT

Oceanographic features such as jets and vortices are often found downstream of obstacles and landforms such as islands or peninsulas. Such features have high spatial and temporal variability and are, hence, interesting but difficult to measure and quantify. This paper discusses an experiment to identify and resolve such oceanographic features in Selat Pauh, in the Straits of Singapore. The deployment formation for multiple robotic vehicles (Autonomous Surface Craft - ASC), the measurement instruments, and the algorithms developed in extracting oceanographic field variables are described. These were based on two ocean field predictions from well-known geophysical flow dynamic models. Field experiments were carried out and comparison of the forecasts with measurements was attempted. To investigate an unexpected behaviour of one ASC, hindcasts with wind effects and simulation with vortex feature extraction on a larger domain with more involved bathymetry were also partially carried out.

KEY WORDS: Marine robotics; adaptive sampling; ocean jets and vortices.

INTRODUCTION

This paper describes work in progress under a research initiative funded by Singapore's National Research Foundation. This has led to the establishment of the Singapore-MIT Alliance for Research and Technology (SMART, 2008) and the creation of MIT's first research center outside the USA. One of the interdisciplinary research projects within SMART is the Center for Environmental Sensing and Modeling (CENSAM, 2008). One component of CENSAM involves oceanographic modeling, forecasting and experimentation with a network of robotic vehicles both surface and underwater. The overall objective of this part of the project is to develop adaptive sampling and assimilation strategies that would enhance our ability to forecast physical, chemical and biological oceanography fields through suitable optimized use of the measurement resources operating in a coupled fashion with computational models of the dynamic ocean behavior. This paper describes recent collaborative research and experiments over the last twelve months, carried out by MIT scientists and engineers and counterparts at the National University of Singapore (NUS). The overall project involves 4 professors, 2 research scientists, 3 postdoctoral associates, 6 research engineers and 2 PhD students.

Oceanographic features such as jets and vortices are often found downstream of obstacles and landforms such as islands or peninsulas and can be also the results of instabilities of jet-like currents (Jochum et al., 2004). Such features have high spatial and temporal variability and are, hence, interesting but difficult to measure and quantify. This paper discusses field experiments to identify and resolve such oceanographic features in the Selat Pauh channel, in the Straits of Singapore. The deployment formation for multiple robotic vehicles - ASC, the measurement instruments, and the algorithms developed in extracting oceanographic features are described. The planning of these experiments at sea was based on two ocean field predictions from well-known geophysical flow dynamic models, one from the Tropical Marine Science Institute (TMSI) of NUS and the other from the Department of Earth, Atmospheric and Planetary Sciences (EAPS Department) at MIT. Field experiments were carried out in January 2009 in the Selat Pauh channel, and comparison of the forecasts with measurements were also carried out in preliminary fashion following basic statistical and spectral analyses of the data. Hindcasts with wind effects and simulation on a larger domain with more involved and accurate bathymetry were also partially carried out followed by the application of a vortex identification algorithm to investigate the unexpected behaviour of one drifting ASC.

This paper is organized as follows. The first section describes the forecasting work and the models employed by TMSI and EAPS. The results of these models were used to plan meaningful field experiments in the Straits of Singapore, that were attached to a more general experimental program under CENSAM in January 2009. The next section describes the field experiments planned and carried out during two days in January 2009. The following section describes the results obtained and comparison of the measurements with forecasts. The paper concludes with recommendations for further work.

SIMULATION AND FORECAST

Field experiments were carried out in the Selat Pauh channel in the Singapore Straits. The dates of the experiments were January 14 and 21, 2009. As the area of operation and dates when the experiments were to be carried out were fixed, forecasts of the oceanic properties in the specific area for the dates of experiments were produced to aid in the design of the experiments to be conducted. Different forecasts of the same day and time were carried out by two independent groups. Both

groups utilized different hydrodynamic models and grids. Details of the simulations are summarized below.

Forecasts by NUS TMSI

The hydrodynamic forecast of the oceanic properties at Selat Pauh is simulated by the nonlinear shallow-water Tropical Marine Hydrodynamic (TMH) model which was developed at NUS TMSI (Pang et al., 2003; Pang and Tkalich, 2004). A regional model, called TMHSSR100, which covers the entire Singapore Straits as well as Eastern and Western Johor Straits with a regular rectangular grid with 100 *m* resolution is first used. In order to obtain a finer resolution of the forecast in the area of operation, a local model, called SP10, that encompasses the area of operation was then run with boundary conditions obtained from the TMHSSR100 model. The model SP10 has a 10 *m* rectilinear grid and covers an area of 4.5 *km* by 6.5 *km* that includes Selat Pauh, as shown in Figs. 1 and 2. *In all figures, the colors represent the bathymetry except otherwise indicated. Blue represents shallow water. Red represents deep water. Olive green represents land.*

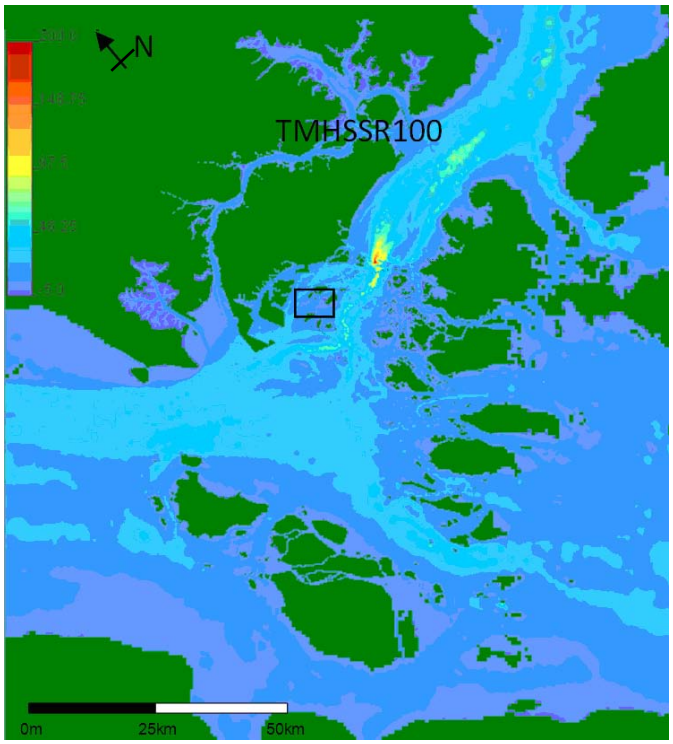

Fig. 1. A bathymetry map of the TMHSSR100 model used by TMSI.

The TMHSSR100 model is driven mainly by tidal elevations at the open boundaries, which also include annual (monsoon-driven) constituents. The prescribed values are based on harmonic constituents derived from TotalTide (UKHO, 2003) and other dedicated measurements in the region. TMHSSR100 boundary conditions have been well calibrated and validated to provide a hydrodynamic forecast in Singapore Straits. River discharges are added in the Eastern part of Johor Strait according to a Delft study (Delft, 2003). Tidal elevation and current velocity from the regional model are imposed at the open boundaries of the local model.

Forecasts by the MIT EAPS Department

The predictions for the tidal circulation for the dates of experiments

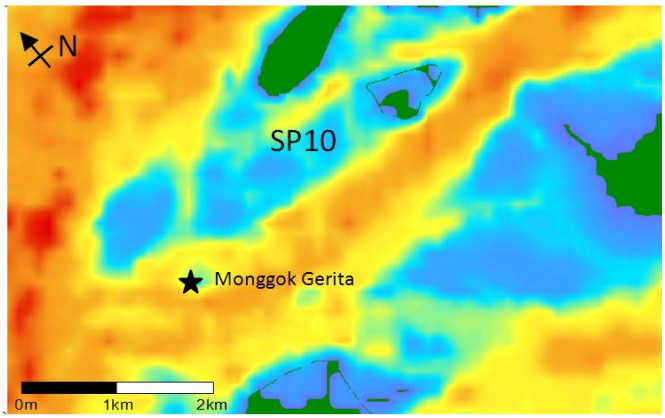

Fig. 2. The local model SP10. Monggok Gerita is a sea-mount that lies in the area of operation in Selat Pauh.

were carried out using the Finite Volume Coastal Ocean Model (FVCOM) (Chen et al., 2003) which adapts non-overlapping unstructured triangular grids to the considered domain. This combines the advantages of finite element methods for geometric flexibility and finite differences methods for computational efficiency. The sigma coordinate was used in the vertical direction for a more accurate representation of the bottom topography. The integration of FVCOM is fully parallelized for multiple processors, which efficiently reduces the computing time for the real application (Cowles, 2008). The channel domain was extracted from a larger domain covering the entire Singapore Strait with six open boundaries. The model was driven by tidal forcing prescribed only at the open boundaries from observations provided by TMSI. From the Singapore Straits domain a circular domain, covering the Selat Pauh channel and all its major islands, was extracted. The horizontal resolution is 500 *m* at the circular open boundary and is increased to 20 *m* along the islands coastlines. The model was driven by the barotropic tide at the circular boundary interpolated from the simulation in the Singapore Strait domain.

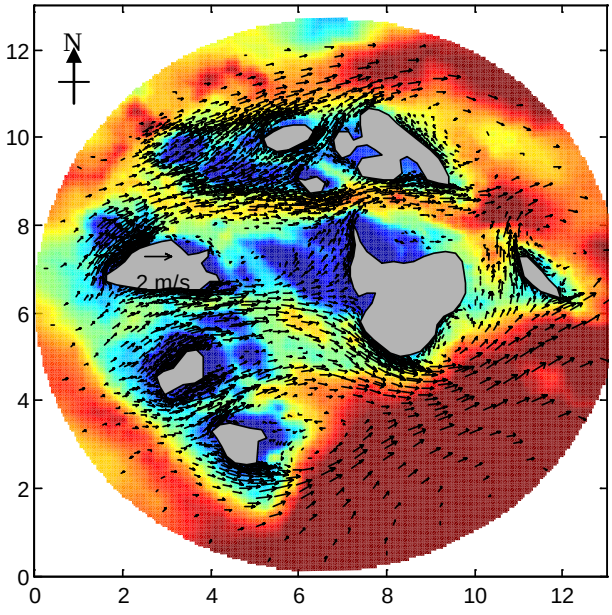

Fig. 3. Forecast for January 21, 2009 carried out with the EAPS model for the tidal circulation in the enlarged Selat Pauh channel and surrounding islands. The origin is at (1.1443^{o} N, 103.6975^{o} E) and the axes are in *km*.

The real tidal observations available at the open boundaries of the Singapore Strait domain cover two periods, June 2006 and January 2007. The elevations for 2006 were reconstructed by harmonic analysis decomposition and fitting to the 2006 tidal record. The tidal prediction was then made for January 2007 and the observations were used for validation. The comparison of predicted and observed elevations for January 2007 showed that the prediction through harmonic analysis is very good. Successively, the surface elevations predicted at the six open boundaries of the Singapore Straits were used to predict the tidal circulation in the circular domain until January 21, 2009. Fig. 3 shows the predicted circulation for January 21, 1300 SST. Fig. 4 shows the same circulation for the region where the experiment was carried out, indicating an overall eastward flowing current. (Wei and Malanotte-Rizzoli, 2009, in preparation).

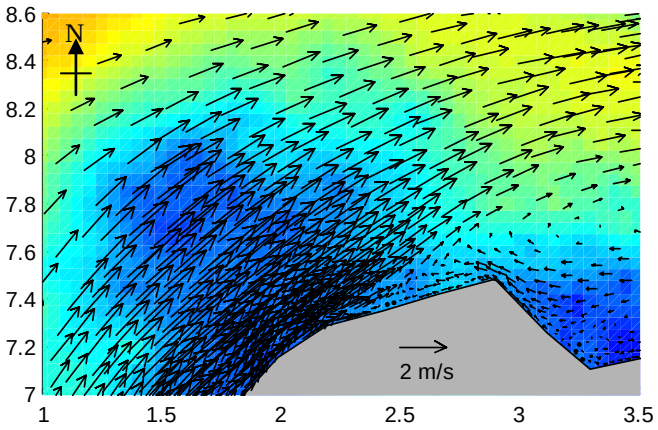

Fig. 4. As in Fig 3, but zooming into the region of the field experiment. The circulation is dominated by an eastward flowing current. The origin is at (1.2072^{o} N, 103.7064^{o} E) and the axes are in *km*.

FIELD EXPERIMENTS

Experiments were conducted in a channel known as Selat Pauh in the Straits of Singapore in January 2009. The area was assigned by the Maritime Port Authority of Singapore (MPAS) and the operations of the vehicles are restricted to the area within the polygon shown Fig. 5.

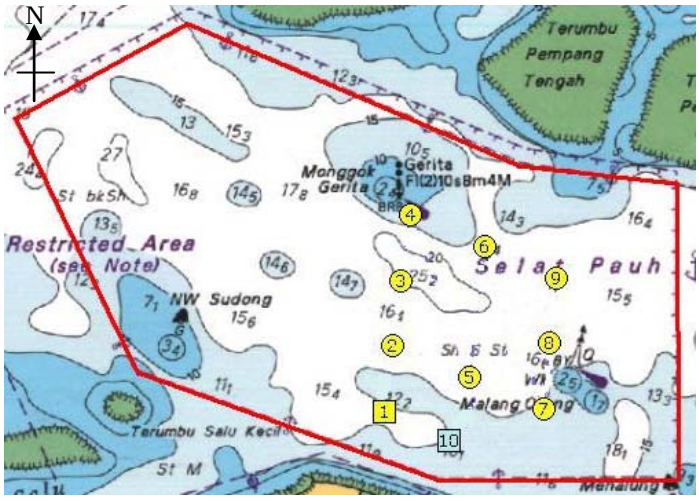

Fig. 5. The permitted area of operation is demarcated by a polygon. Points labeled 1 to 10 are starting points and waypoints used in the tests. Map is obtained from MPAS.

In total, three ASC were available for deployment. The ASC (*3m* long and *0.8m* wide) are able to work at a maximum operational speed of 2m/s with full load for 3 hours and are controlled either by the computers mounted in the hull or remote controllers. To differentiate the ASC, they are labeled as 'Blue', 'Red' and 'White'. Two of the ASC, the blue and red ASC, had paddle wheel sensors while the other has a Doppler Velocity Log (DVL) instead of a paddle wheel sensor. The paddle wheel sensor, manufactured by Furuno (model name 235DST-PSE), measures the speed of the ASC with respect to the water in the centerline direction of the ASC. Global Positioning Systems (GPS) and compasses were mounted on all the three ASC to track and control the movement of the ASC and measure the heading of the ASC respectively. With the measurements from the GPS and compasses and paddle wheel sensors, the velocity of the surface current can be estimated. The GPS, model name 18x, manufactured by Garmin had an accuracy of up to 3 *m*. The sampling frequency is 5 *Hz*. The compass, model name OS5000, manufactured by Ocean Server could measure the azimuth angle up to an accuracy of 0.5^{o}.

Although the dates of the experiments were fixed, the time at which the vehicles would be deployed to obtain measurements could be selected. Forecasts of the currents in the area of operation for January 14 and 21 were used to plan experiments that would measure interesting oceanic features that had dynamic variability. Results from the forecast from TMSI for January 14 indicated the presence of a jet that was due to an island, known as Pulau Hantu that was upstream of the area of operation as shown in Fig. 6. The jet was observed when currents were flowing from East to West at around 1000 to 1230 SST.

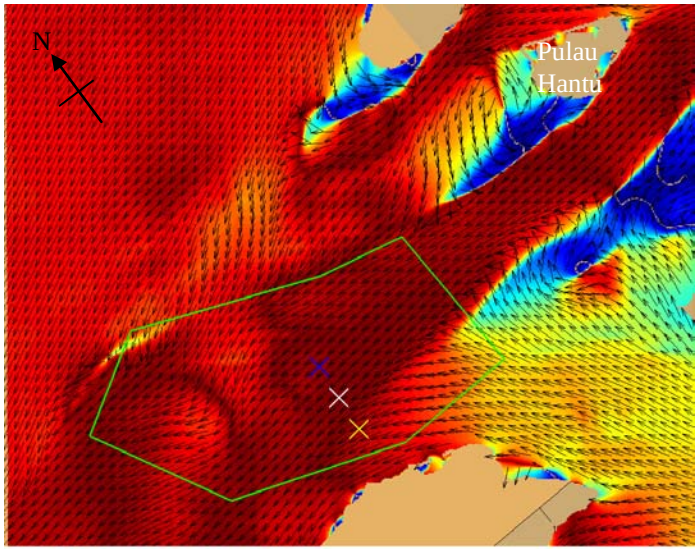

Fig. 6. The result of the forecast for January 14. The green polygon demarcates the area of operations. A jet caused by Pulau Hantu island is observed in the area of operation. The 'x's mark the starting points of the ASC for the drifting test, which will be described in detail below. The color contours represent the magnitude of the forecasted velocity. Arrows are all of unit magnitude and only indicate the direction of the velocity.

There was lack of dynamic variability in the currents from the forecast of January 21. However, based on the charts of the forecast at a point that lies within the area of operation, as shown in Fig. 7, the interval at about noon was chosen as the time to conduct the experiment. The tests conducted on January 21 were similar to those of January 14 to enhance the confidence of the tests conducted on January 14. In addition, a different test was carried out to evaluate the performance of the sensors on the ASC. Detailed descriptions of the tests are below.

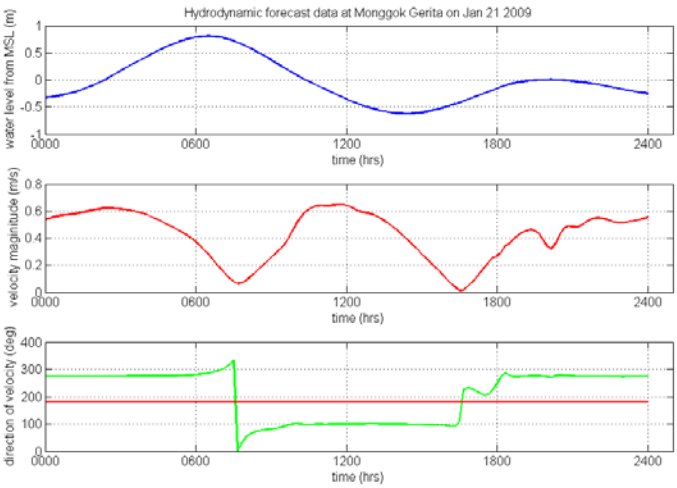

Fig. 7. The hydrodynamic forecast for January 21, 2009 at Monggok Gerita (1.2236^{o} N, 103.7240^{o} E). The maximum speed of the current occurs around 1200 SST. The direction of the velocity is measured clockwise from the North.

Test Descriptions

Three different tests were designed for the entire experiment. The tests are known as 'drifting test', 'cross test' and 'upstream test'. The drifting and cross tests were carried out on both days while the upstream test was carried out only on January 21. One ASC in operation is shown in fig. 8 below.

Fig. 8. An ASC with a red flag (called red kayak in this paper) in operation

For the drifting test, the ASC were allowed to drift along with the currents without power from their engine. The cross test was designed such that the ASC run almost orthogonal to the direction of the forecasted velocity of the current. The upstream test comprises of the ASC running almost parallel and opposite to the direction of the forecasted velocity of the current. With reference to Fig. 5, Table 1 summarizes the position of the starting points and waypoints of the various tests.

Table 1. Summary of the position of the starting points and waypoints for the tests conducted in January 2009.

Test	ASC Color	Starting point	Terminating point
Drifting	Red	1	-
	White	2	-
	Blue	3	-
Cross	Red	2	4
	White	5	6
	Blue	7	9
Upstream	Red	7	1
	White	8	2
	Blue	9	3

Drifting Test

In the drifting test, the ASC are first driven under power to their respective starting position. The starting positions, as shown in Fig. 6, were chosen to lie within the jet that was observed from the forecast from TMSI. The ASC were deployed from a controller ship one by one and were driven under power to their designated starting position. ASC that have arrived at their starting position were driven under power to remain at position until the other ASC reached their destinations. Once all the ASC were in their designated starting position, the power to their engines was cut simultaneously for the ASC to drift along with the current, starting at the same time.

Cross Test

Two waypoints were chosen such that the ASC traversed between these two points and the trajectory produced by the ASC will be nearly orthogonal to the direction of the forecasted velocity of the current. The paths of the ASC were designed such that there were nearly parallel to each other as the waypoints are as shown in Fig. 5. The ASC started from their South waypoints simultaneously and were driven under power to travel to their North waypoints.

Upstream Test

Similar to the cross test, the upstream test requires two waypoints to be selected for the ASC to traverse between. However, these waypoints were chosen such that the trajectories of the ASC are now nearly parallel to the direction of the forecasted velocity of the current. This test was only conducted on January 21 and referring to Fig. 6, the current was forecasted to flow from West to East during the test. Hence, the starting positions of the ASC were picked to be the East waypoints, as shown in Fig. 5, for the ASC to travel upstream when they head towards the West waypoints. This enabled the paddle wheel sensor to measure data most meaningfully as it is nearly aligned to the direction of the current.

RESULTS AND DISCUSSION

The results and analysis for the drifting test for both test days and the upstream test on January 21 will be presented in the following subsections.

Results from January 14

The drifting test was conducted from 1052 to 1105 SST, within the interval that the jet was forecasted. Fig. 9 shows the trajectory of the three ASC. The colors of the paths correspond to the respective ASC. The magenta arrows are the forecasted velocity of the currents and the black arrows represent the velocity of the current computed by measurements from the paddle wheel sensor, GPS and compass. Qualitatively, the trajectory and measured velocity is in good agreement with the forecasted velocity.

Charts of the measured and forecasted speed and heading are shown in Figs. 10 and 11, respectively. The root-mean-squared (rms) difference between the measured and forecasted speed is 0.72 of the mean of the forecasted speed, while the rms difference between the measured and forecasted direction of the velocity is -0.13 of the mean of the forecasted direction. Hence, the measured and forecasted velocities of the current do not differ much in direction but have some significant difference in magnitude.

The results obtained from the cross test do not agree as well as the results from the drift test and analysis is currently being done to understand the reasons for the errors. As the limitation of the paddle wheel sensor to measure in only a single direction is suspected as one of the causes of the errors, the upstream test was conducted on January 21 to evaluate the performance of all the equipment, especially the paddle wheel sensor.

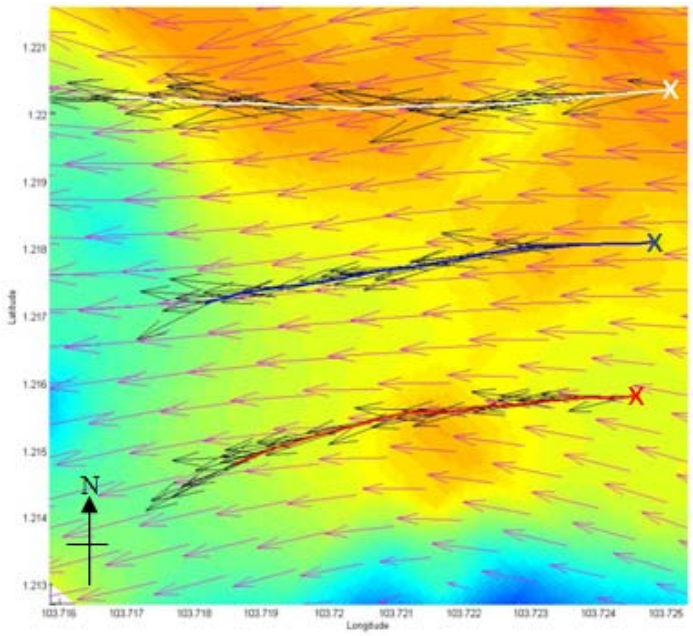

Fig. 9. A plot of the trajectories of the ASC for the drifting test on January 14. The ‘x’s mark the starting position of the ASC. The magenta arrows are the forecasted velocities of the currents. The black arrows are the computed velocities of the current based on measurements.

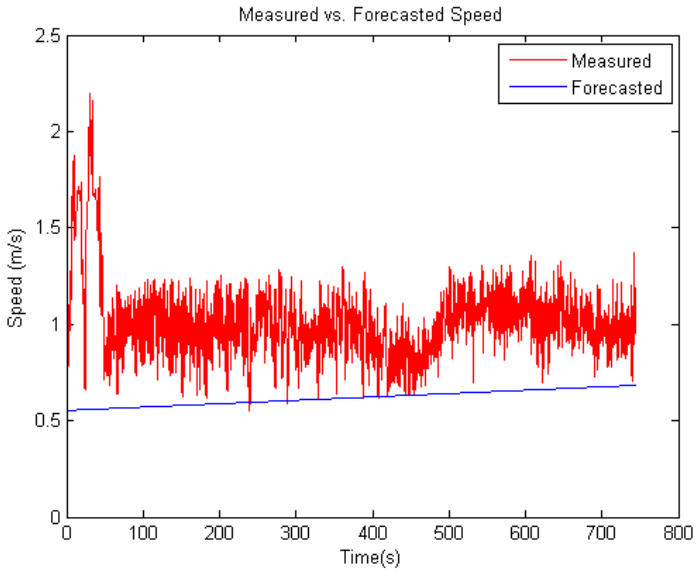

Fig. 10. A plot of speed vs. time for the measured speed (in red) and the forecasted speed (in blue) for the drifting test on January 14. These measurements come from the red ASC.

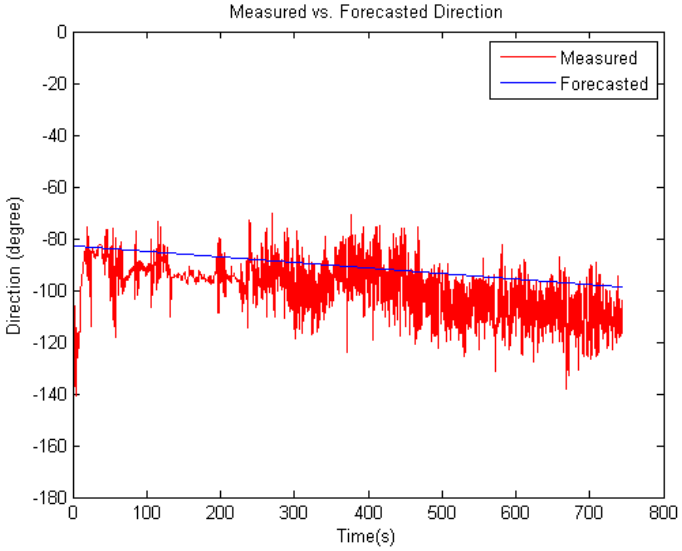

Fig. 11. A plot of heading vs. time for the measured heading (in red) and the forecasted direction (in blue) for the drifting test on January 14. The angle measured clockwise from the North. These measurements come from the red ASC.

Results from January 21

Upstream Test

The upstream test was conducted to evaluate the performance of all the equipment, in particular the paddle wheel sensor. The test was conducted from 1353 to 1359 SST. A plot of the measured and forecasted speed against time and a plot of the measured and forecasted direction of the velocity of the current are shown in Figs. 12 and 13 respectively. The rms difference between the measured and forecasted speed is 0.59 of the mean of the forecasted speed. The rms difference between the measured and forecasted direction of the velocity is 0.14 of the mean of the forecasted direction. Hence, the measured and

forecasted velocities of the current do not differ much in direction but have some significant difference in magnitude.

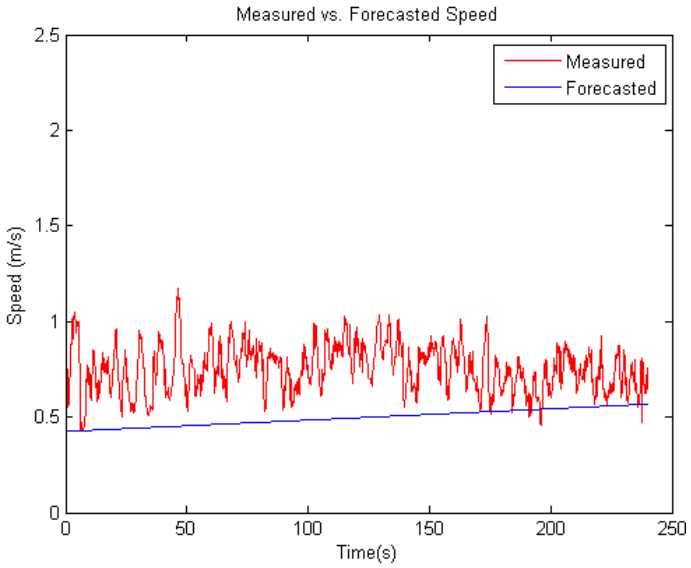

Fig. 12. A plot of speed vs. time for the measured speed (in red) and the forecasted speed (in blue) for the upstream test on January 21. These measurements come from the red ASC.

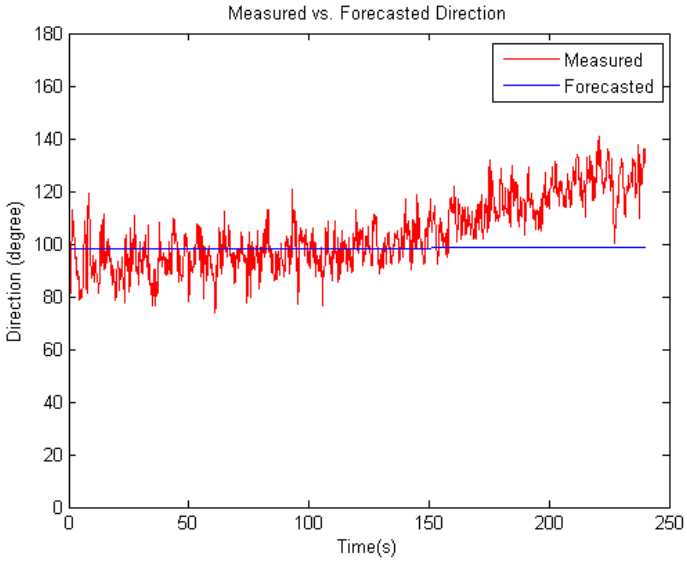

Fig. 13. A plot of heading vs. time for the measured heading (in red) and the forecasted direction (in blue) for the upstream test on January 21. The angle measured clockwise from the North. These measurements come from the red ASC.

Drifting Test

The drifting test for January 21 was conducted from 1258 to 1308 SST. The quantitative result of the drifting test is shown in Fig. 14. The red and white ASC drifted towards the East, along the direction of the forecasted current. However, the blue ASC displayed an unexpected behavior by drifting towards a South-South-Westerly direction when the forecasted direction of the current at its location was from West to East.

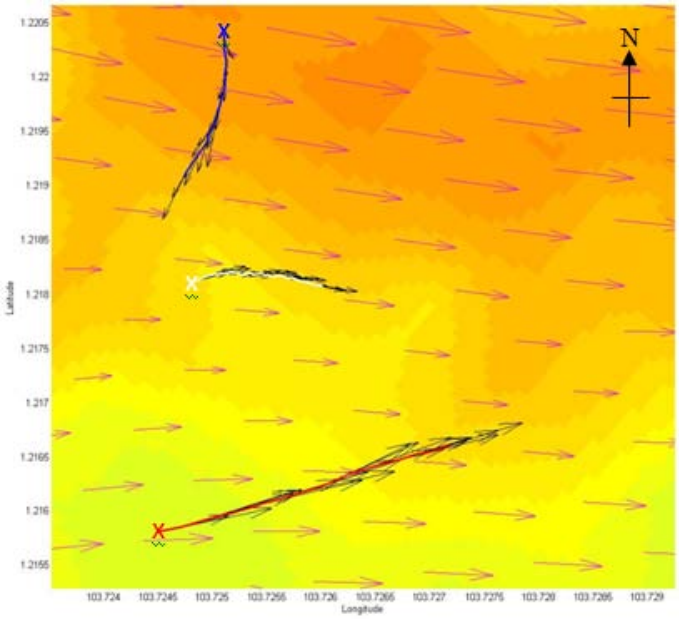

Fig. 14. A plot of the trajectories of the ASC for the drifting test on January 21. The 'x's mark the starting position of the ASC. The magenta arrows are the forecasted velocities of the currents. The black arrows are the computed velocities of the current based on measurements obtained.

The true cause of the unforeseen behavior of the blue ASC is not certain but some hypotheses have been put forward and are explained below.

Hypothesis

Many hypotheses, such as the effect of wind, finer bathymetry resolution and computational domain for the forecast, have been proposed to be the possible cause for the unexpected behavior of the blue ASC for the drifting test on January 21. A likely reason for the disagreement between the behavior of the blue ASC and the forecast velocity of the current was the computational domain of the forecast. There is a region of shallow water (2m deep on the average) around P. Salu north-west of the island of Pulau Sudong, as shown in Fig. 15, which had not been included in the smaller, higher resolution computational domain of the TMH model. When the larger computational domain was used in the model, eddy systems behind P. Salu and P. Sudong that had not been observed with the smaller computational domain were present in the area of operation as shown in Figs. 16 and 17. A vortex detection algorithm was carried out on the results of the forecast for the larger domain. The algorithm is a set-based vortex detection method utilizing geometric properties of vortices including direction spanning (Guo et al. 2004) and winding angle (Sadarjoen and Post 2000) properties. It also employs a method, commonly referred to as λ_2-method (Jeong and Hussain 1995), to filter out false candidates.

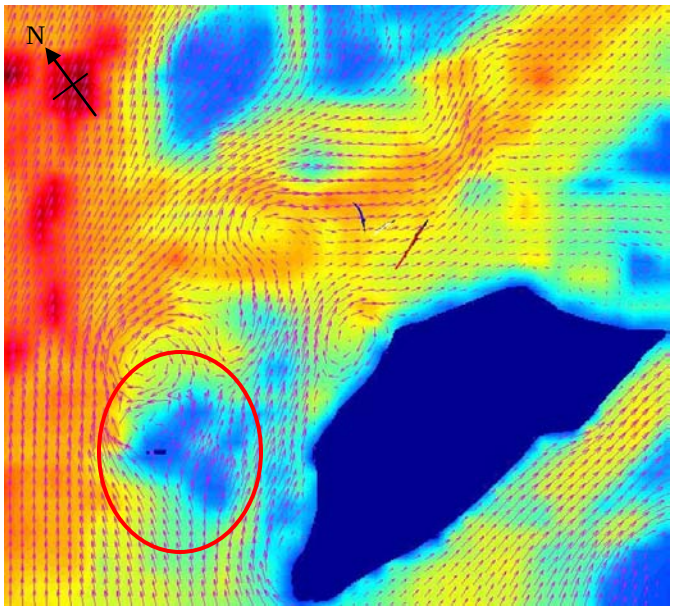

Fig. 15. The red ellipse emphasizes the shallow water region around P. Salu which lies northwest of Pulau Sudong that was left out of the smaller computational domain. The blue, white and red lines are the trajectories of the ASC for the drifting test from January 21.

Figs. 17 and 18 can justify the behavior of the white and red ASC depicted in green and red lines, respectively. The paths of the white and red ASC describe their drifting along the predicted west-to-east current flow. Furthermore, the vortex street observed behind the P. Salu (see Fig. 17) can account for the unexpected behavior of the blue ASC drifting towards south (although the simulated phase of the vortex shedding does not exactly coincide with the measurement). In addition, the authors plan to carry out data assimilation based on the experimental results.

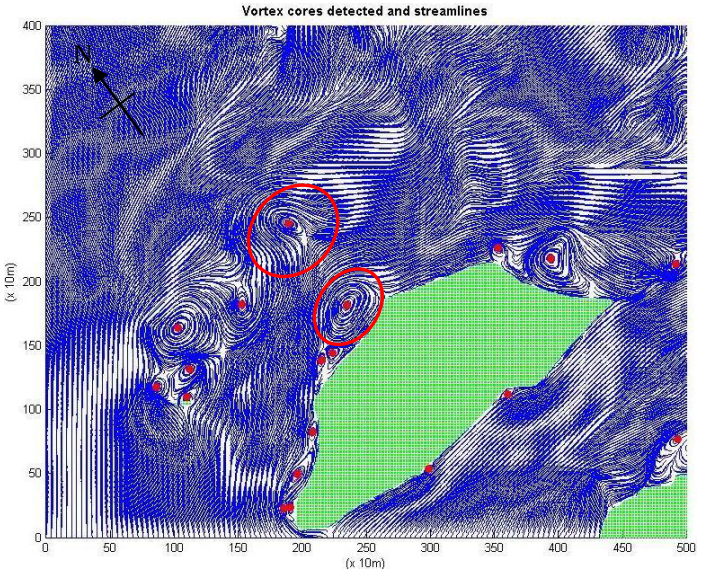

Fig. 16. Vortex cores identified (solid red circles) and streamlines in Selat Pauh including two (surrounded by red ovals) near the drifting test area at 1300 SST, January 21, 2009.

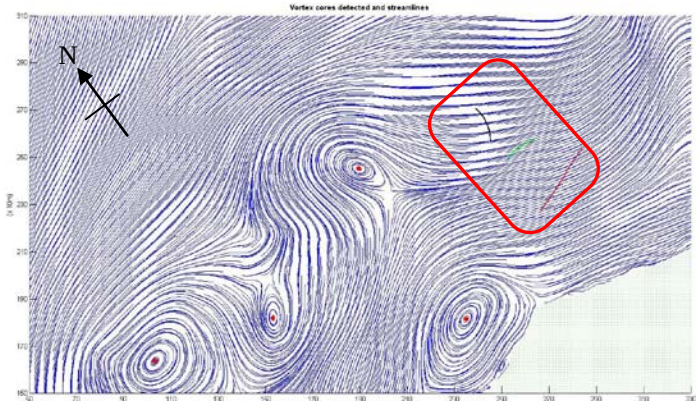

Fig 17. A zoom-in to the drifting test region near P. Sudong and P. Salu. Paths of the three ASC are also shown in blue, green and red lines surrounded by a red box.

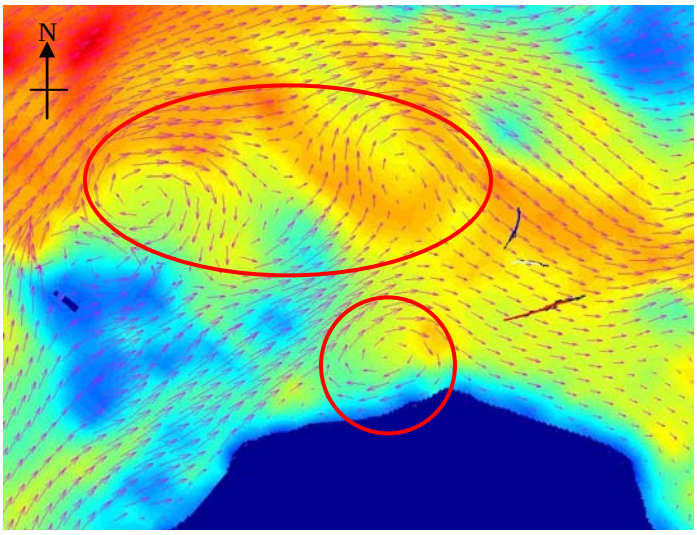

Fig. 18. A zoom-in to the area near the starting position of the ASC for the drifting test on January 21. A smaller red circle emphasizes the presence of a vortex behind P. Sudong, and a region marked by a bigger ellipse (together with Figs. 16, 17) shows the vortex street behind P. Salu and their effect on the unexpected behaviour of the blue ASC.

As briefly mentioned before, more hypotheses including the wind effect have been proposed to investigate the unexpected behavior of the blue ASC in a drifting mode. However, it is unlikely that the effect of the wind can produce as marked a difference in the drifter's trajectory as that observed. In order to make a preliminary assessment of the effects of the wind on the movement of the ASC, a hind-cast of the ocean currents in the area of operation was carried out using the MIT/EAPS model with the larger computational domain shown in Fig. 15 and including a time averaged value of the wind velocity. This value was obtained by anemometer on the deck of the controller ship anchored at the (1.2148^0 N, 103.7268^0 E). The mean wind magnitude was computed to be 3.95 *m/s* and the mean direction was 40.32^0 from the North in a clockwise direction.

Fig. 19 shows the resulting circulation zooming-in the area near the starting position of the ASC for the drifting test of January 21. The ASC positions are marked. With the enlarged domain capturing the region of shallow water north-west of the Pulau Sudong island, the

EAPS model also captures two vortices similarly described in the preceding plots based on the TMH model. Fig. 20 shows the residual wind-driven circulation in the same zoomed-in region. The wind driven velocity is one order of magnitude smaller than the total one and is therefore rather weak. Further dynamic analysis of wind force on the ASC corroborates this. The average total force on the kayak estimated from acceleration rate is 62 N approximately in the North-South direction while the wind force on the kayak from aerodynamics calculation is approximately 4.9 N in the North-South direction. This shows that the influence of the wind on the motion of the ASC is insignificant.

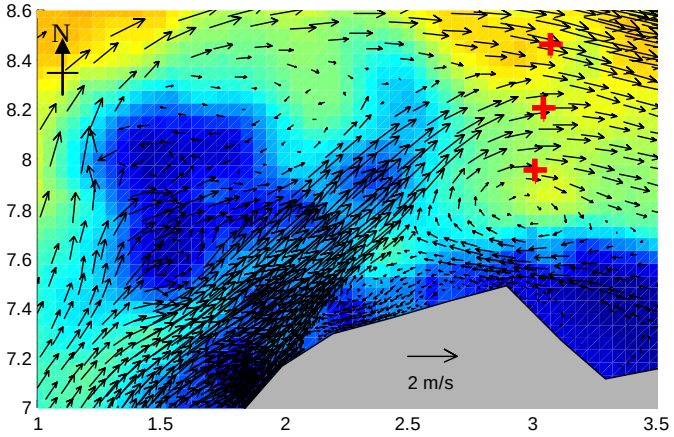

Fig. 19. Hind-cast of the tidal and wind-driven circulation at 1300 SST of January 21, zooming in the region of the ASC experiment. The ASC initial positions are marked. Two vortices similarly described in the preceding plots are also evident. The origin is at (1.2072^o N, 103.7064^o E) and the axes are in *km*.

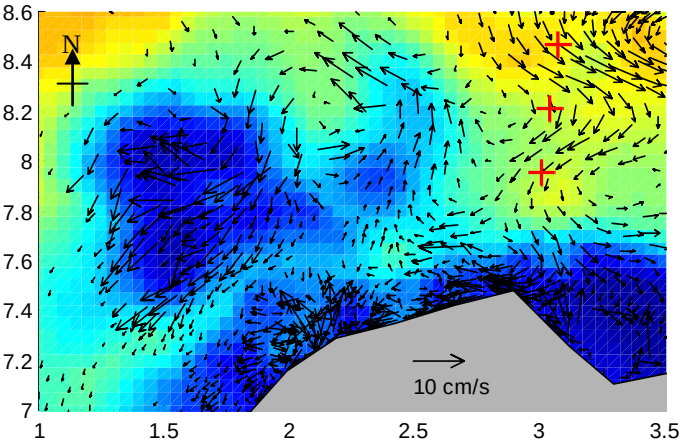

Fig. 20. The residual wind-driven circulation at 1300 SST of January 21 in the same region as in Fig. 19. The origin is at (1.2072^o N, 103.7064^o E) and the axes are in *km*.

CONCLUSIONS AND FUTURE WORK

Experiments were conducted in a narrow channel in the Singapore Straits known as Selat Pauh. Three ASC were used to conduct three different experiments on January 14 and January 21, 2009. The experiments designed were based on forecasts of the ocean currents from the NUS TMSI and MIT EAPS Departments.

Results of the measured current velocity from the drifting test for January 14 and the upstream test for January 21 agrees well with the predicted current velocity. The blue ASC displayed an unexpected behavior in the drifting test of January 21 and possible hypotheses for this phenomenon have been studied. A combination of numerical simulation with accurate bathymetry map, higher spatio-temporal resolution, and data assimilation techniques would greatly assist in improving the ability of computational models to accurately identify the field with interesting oceanographic features.

ACKNOWLEDGEMENTS

The authors would like to thank Prof. F. S. Hover, Dr. A. Tan, Dr. T. Bandyopadhyay for their assistance in planning and executing the January 2009 sea trials. The assistance provided by Ms. L. M. Sarcione and Mr. A. N. R. Patrikalakis in the executions and operations of the ASC in the sea trials is appreciated. Funding for this work was obtained by a grant from the Singapore National Research Foundation under the SMART/CENSAM initiative (CENSAM, SMART, 2008).

REFERENCES

CENSAM 2008, http://censam.mit.edu.

Chen, C, Liu, H and Beardsley, RC (2003). *"An unstructured, finite-volume, three-dimensional, primitive equation ocean model: application to coastal ocean and estuaries,"* J. Atmos. Oceanic Tech., 20, pp 159-186.

Cowles, GW (2008). *"Parallelization of the FVCOM coastal ocean model,"* Int. J. High Perform. Comput. Appl., 22(2), pp 177–193.

Delft (2003). *"Hydraulic Model Studies for Pulau Tekong Reclamation Scheme,"* WL|Delft Hydraulics.

Guo, D, Evangelinos, C, and Patrikalakis, NM (2004). *"Flow Feature Extraction in Oceanographic Visualization,"* Computer Graphics International Conference, CGI 2004, D. Cohen-Or, L. Jain and N. Magnenat-Thalmann, editors. pp. 162-173. Crete, Greece, June 2004. Los Alamitos, CA: IEEE Computer Society Press.

Jeong, J and Hussain, F (1995). *"On the Identification of a Vortex,"* J. Fluid Mechanics, 285:69-94.

Jochum, M, Malanotte-Rizzoli, P and Busalacchi, AJ, (2004). "Tropical instabilities waves and vortices in the Atlantic Ocean,"Ocean Modeling, 7, 145-163.

Pang, WC and Tkalich, P (2004). *"Semi-Implicit Sigma-Coordinate Hydrodynamic Model,"* Proc. 14th IAHR-APD Congress. 15 - 18 Dec. 2004, Hong Kong.

Pang, WC, Tkalich, P and Chan, ES (2003). *"Hydrodynamic forecast model for the Singapore Straits,"* Proc. of the XXX IAHR Congress. August 2003, Thessaloniki, Greece. A: 9-16.

Sadarjoen, A. and Post, F. H. (2000). *"Detection, quantification, and tracking of vortices using streamline geometry,"* Visualization and Computer Graphics, vol. 24, pp. 333–341.

SMART 2008, http://web.mit.edu/smart/

United Kingdom Hydrographic Office (2003). *"Admiralty Total Tide 2003,"* United Kingdom.

Wei, J and Malanotte-Rizzoli, P (2009). *"Tidal circulation forecasts for January 2009 in the Selat Pauh Region,"* in preparation.